2013 European Control Conference (ECC)
July 17-19, 2013, Zürich, Switzerland.

3-D Inertial Trajectory and Map Online Estimation: Building on a GAS Sensor-based SLAM filter

Pedro Lourenço, Bruno J. Guerreiro, Pedro Batista, Paulo Oliveira, and Carlos Silvestre

Abstract— **This paper addresses the problem of obtaining an inertial trajectory and map, with the associated uncertainty, using the sensor-based map provided by a globally asymptotically stable SLAM filter. An optimization problem with a closed-form solution is formulated, and its uncertainty description is derived resorting to perturbation theory. The combination of the algorithm proposed in this paper with the sensor-based SLAM filter results in a complete SLAM methodology, which can be directly applied to unmanned aerial vehicles (UAVs). Both simulation and preliminary experimental results, using an instrumented quadrotor equipped with a RGB-D camera, are included in this work to illustrate the performance of the proposed algorithm under realistic conditions.**

I. Introduction

Navigation and positioning systems are of the utmost importance in the development of unmanned aerial vehicles (UAVs). Particularly in mission scenarios where georeferencing is not possible, either indoors or outdoors, relative positioning systems are fundamental to accomplish any given mission, avoid collisions, or even to maintain stability. This paper presents an algorithm, which can be used within the scope of simultaneous localization and mapping (SLAM) [1], to address the problem of estimating the trajectory and map, in a generic inertial reference frame, using only sensor-based map information.

The authors have devised a novel dual strategy to tackle the problem of developing an online SLAM algorithm for unmanned aerial vehicles with global convergence properties. This strategy encompasses 1) a sensor-based SLAM filter which estimates the landmark map, the linear velocity and the angular measurement bias expressed in the body-fixed frame [2]; and 2) an Inertial Trajectory and Map (ITM) estimation algorithm resulting from an optimization problem with closed-form solution, which uses the sensor-based map estimate of the SLAM filter, and provides a fully characterized uncertainty approximation for this highly nonlinear problem. This approach generalizes the dual algorithm for the bidimensional case proposed in [3] and [4].

The framework of the sensor-based SLAM filter is completely independent of the inertial frame, as every input and state are expressed in the body-fixed frame. Therefore, the localization of the vehicle is trivial, corresponding to the origin of the body-fixed frame, and the sensor-based map is readily available. Nevertheless, most SLAM algorithms perform the mapping and localization in an inertial reference frame, as many applications require the inertial map and the trajectory of the vehicle. In the proposed dual strategy algorithm the pose of the vehicle can be estimated by the comparison of the sensor-based and previous inertial maps. The problem of computing the transformation that maps two sets of points is usually called the Procrustes Problem [5]. Its generalization for rotation, translation and scaling has been subject of extensive research in areas such as computer vision applications and scan-matching, and can be traced back to [6] and [7]. The statistical characterization of this problem has also been the subject of study in works such as [5], [8], and [9]. However, some rather limiting options were taken, namely, the absence of weighting of the point sets, the use of small rotations, or the same covariance for all landmarks. This work proposes a methodology for obtaining the inertial map and the pose of the vehicle corresponding to a body-fixed map produced by a sensor-based SLAM filter, which builds on the work presented in [4], by extending the formulation of the orthogonal Procrustes problem therein to three dimensions, and providing the uncertainty characterization of the obtained transformation. This is achieved resorting to perturbation theory, by considering arbitrary rotations and translations, individual weights, and individual covariance matrices for the landmarks of the inertial map.

The paper is organized as follows: Section II presents an overview of the sensor-based SLAM filter that complements this work. In Section III, the Procrustes problem is defined as an optimization problem solved in a closed-form, and the uncertainty of the solution is described. The ITM algorithm is described in Section IV, from the problem formulation to the uncertainty characterization. The simulation results are presented in Section V and preliminary experimental results using an instrumented quadrotor are detailed in Section VI. Finally, concluding remarks and some directions for the future are presented in Section VII.

Notation: The superscript ^{I} indicates a vector or matrix expressed in the inertial frame $\{I\}$. For the sake of clarity, when no superscript is present, the vector is expressed in the body-fixed frame $\{B\}$. $\mathbf{I}_n$ is the identity matrix of dimension $n \times n$, and $\mathbf{0}_{n\times m}$ is a n by m matrix filled with zeros. If m is omitted, the matrix is square. $\mathbf{S}[\mathbf{a}]$ is a special skew-symmetric matrix, henceforth called the cross-product matrix, as $\mathbf{S}[\mathbf{a}]\mathbf{b} = \mathbf{a} \times \mathbf{b}$ with $\mathbf{a}, \mathbf{b} \in \mathbb{R}^3$. The matrix norm of a generic matrix $\mathbf{A}$ is defined as the Frobenius norm $\|\mathbf{A}\|^2 = \mathrm{tr}\left(\mathbf{A}\mathbf{A}^T\right)$, and the determinant is denoted as $\det(\mathbf{A})$. The expected value of any quantity is denoted by the symbol $\langle . \rangle$.

II. Overview

The algorithm proposed in this paper was designed to complement a sensor-based SLAM filter, as part of a SLAM algorithm that provides estimates in both the body-fixed

This work was partially supported by the FCT [PEst-OE/EEI/LA0009/2011], and by project FCT AMMAIA (PTDC/HIS-ARQ/103227/2008).

The authors are with the Institute for Systems and Robotics, Instituto Superior Técnico, Universidade Técnica de Lisboa, Av. Rovisco Pais, 1049-001 Lisboa, Portugal. Carlos Silvestre is also with the Department of Electrical and Computer Engineering, Faculty of Science and Technology of the University of Macau.

{plourenco,bguerreiro,pbatista,pjcro,cjs}@isr.ist.utl.pt

frame and the local inertial frame. A brief description of the sensor-based filter is provided in this section, as an introduction to the ITM algorithm detailed later in this paper. This sensor-based SLAM filter was introduced in [2] and consists of a Kalman filter for the system

$$\begin{cases} \dot{\mathbf{x}}(t) = \mathbf{A}(t, \mathbf{x}_M(t))\mathbf{x}(t) \\ \mathbf{y}(t) = \mathbf{x}_O(t) \end{cases}, \tag{1}$$

with

$$\mathbf{A}(t, \mathbf{x}_M(t)) = \begin{bmatrix} \mathbf{0}_{6\times3} & \mathbf{0}_{6\times3} & \mathbf{0}_{6\times3} & \cdots & \mathbf{0}_{6\times3} \\ -\mathbf{I}_3 & -\mathbf{S}\left[\mathbf{p}_1(t)\right] & -\mathbf{S}\left[\boldsymbol{\omega}_m(t)\right] & \cdots & \mathbf{0}_3 \\ \vdots & \vdots & \vdots & \ddots & \vdots \\ -\mathbf{I}_3 & -\mathbf{S}\left[\mathbf{p}_{N_M}(t)\right] & \mathbf{0}_3 & \cdots & -\mathbf{S}\left[\boldsymbol{\omega}_m(t)\right] \end{bmatrix},$$

where $\mathbf{p}_i(t) \in \mathbb{R}^3$ represents a landmark, $\omega_m(t) \in \mathbb{R}^3$ is the noisy and biased angular velocity, the state $\mathbf{x}(t)$ is composed by the linear velocity and the angular measurement bias as well as with the landmark based state $\mathbf{x}_M(t)$, all expressed in body-fixed coordinates, and the output is composed by the visible landmarks.

Relieving (1) of the non-visible landmarks yields a system that is shown to be uniformly completely observable, allowing the design of the globally asymptotically stable filter in [2] that provides estimates of the sensor-based map and its uncertainty, which are used in what follows to obtain the inertial trajectory and map estimation algorithm proposed.

III. Procrustes Problem

This section addresses the extended orthogonal Procrustes problem. An optimization problem is formulated using individual weights and a closed-form solution is found. Furthermore, the uncertainty characterization of the obtained translation and rotation is also performed.

A. Optimization Problem and Closed-form Solution

Consider the existence of two landmark sets, $\mathcal{L}_A$ and $\mathcal{L}_B$, which contain, respectively, the landmarks expressed in an arbitrary frame $\{A\}$ and the same landmarks expressed in some other frame $\{B\}$. Each landmark $\mathbf{a}_i \in \mathcal{L}_A$ corresponds to a landmark $\mathbf{b}_i \in \mathcal{L}_B$, with $i \in \{1, \ldots, N_{\mathcal{L}}\}$, and that correspondence is expressed by $\mathbf{a}_i = \mathbf{R}\mathbf{b}_i + \mathbf{t}$, where the pair $(\mathbf{R}, \mathbf{t}) \in \mathrm{SO}(3) \times \mathbb{R}^3$ fully defines the transformation from frame $\{B\}$ to frame $\{A\}$, as it represents the rotation and translation from $\{B\}$ to $\{A\}$. Obtaining the pair $(\mathbf{R}, \mathbf{t})$ is the purpose of the optimization problem

$$(\mathbf{R}^*, \mathbf{t}^*) = \arg \min_{\substack{\mathbf{R} \in \mathrm{SO}(3) \\ \mathbf{t} \in \mathbb{R}^3}} G\left(\mathbf{R}, \mathbf{t}\right), \tag{2}$$

where the functional $G\left(\mathbf{R}, \mathbf{t}\right)$ is defined as

$$G\left(\mathbf{R}, \mathbf{t}\right) = \frac{1}{N_{\mathcal{L}}} \left\| \left(\mathbf{Y} - \mathbf{R}\mathbf{X} - \mathbf{t}\mathbf{1}^T\right) \boldsymbol{\Sigma}_e^{-1/2} \right\|^2,$$

that is the sum of the norm of the error $\mathbf{e}_i = \mathbf{a}_i - \mathbf{R}\mathbf{b}_i - \mathbf{t}$ over $\{1, \ldots, N_{\mathcal{L}}\}$ weighted with $\sigma_i^2 > 0$, $i \in \{1, \ldots, N_{\mathcal{L}}\}$, which account for the intrinsic uncertainty of each landmark pair. $\mathbf{Y} = [\mathbf{a}_1 \quad \cdots \quad \mathbf{a}_{N_{\mathcal{L}}}]$ and $\mathbf{X} = [\mathbf{b}_1 \quad \cdots \quad \mathbf{b}_{N_{\mathcal{L}}}]$ are, respectively, the concatenation of the landmark vectors expressed in frames $\{A\}$ and $\{B\}$, $\mathbf{1} = [1 \quad \cdots \quad 1]^T \in \mathbb{R}^{N_{\mathcal{L}}}$ is a vector of ones, and the weight matrix $\boldsymbol{\Sigma}_e$ is a diagonal matrix whose entries are the weights $\sigma_1^2, \ldots, \sigma_{N_{\mathcal{L}}}^2$ that model the landmark uncertainty. These can be conservatively chosen as $\sigma_i^2 = \lambda_{max}\left(\boldsymbol{\Sigma}_{a_i}\right) + \lambda_{max}\left(\boldsymbol{\Sigma}_{b_i}\right)$ as the true $\boldsymbol{\Sigma}_e$ is not known. This weight matrix allows the use of the information regarding the different degrees of uncertainty of each landmark pair.

The optimization problem here described has a closed-form solution based on the work exposed in [6], [10] , and [5]. The optimal translation vector is

$$\mathbf{t}^* = \frac{1}{N_W}\left(\mathbf{Y} - \mathbf{R}^*\mathbf{X}\right)\boldsymbol{\Sigma}_e^{-1}\mathbf{1} = \boldsymbol{\mu}_A - \mathbf{R}^*\boldsymbol{\mu}_B. \tag{3}$$

Notice that the optimal translation is the vector that translates the weighted centroid of the landmarks in $\mathcal{L}_B$ $\boldsymbol{\mu}_B$, rotated to frame $\{A\}$ to the weighted centroid of the landmarks in $\mathcal{L}_A$, $\boldsymbol{\mu}_A$. For computing the optimal rotation, consider the matrix

$$\mathbf{B} := \mathbf{X}\mathbf{W}\mathbf{Y}^T$$

where $\mathbf{W} := \boldsymbol{\Sigma}_e^{-1} - \frac{1}{N_W}\boldsymbol{\Sigma}_e^{-1}\mathbf{1}\mathbf{1}^T\boldsymbol{\Sigma}_e^{-1}$ and $N_W := \mathbf{1}^T\boldsymbol{\Sigma}_e^{-1}\mathbf{1}$. The singular value decomposition of $\mathbf{B}^T$,

$$\mathbf{U}\mathbf{D}\mathbf{V}^T = \mathrm{svd}(\mathbf{B}^T),$$

is important in finding the optimal rotation that is given by

$$\mathbf{R}^* = \mathbf{U}\,\mathrm{diag}\left(1, 1, |\mathbf{U}|\,|\mathbf{V}|\right)\mathbf{V}^T. \tag{4}$$

B. Uncertainty Characterization

The solution of the optimization problem now defined involves uncertainty at the input and output level: 1) the landmark sets used to estimate the transformation between frames are not exact, having a non-deterministic part; and, thus, 2) the estimated translation and rotation are also non-deterministic. Within the scope of perturbation theory, the error models of the known variables are defined as,

$$\mathbf{a}_i = \mathbf{a}_i^{(0)} + \epsilon\,\mathbf{a}_i^{(1)} + \mathcal{O}(\epsilon^2) \tag{5a}$$

$$\mathbf{b}_i = \mathbf{b}_i^{(0)} + \epsilon\,\mathbf{b}_i^{(1)} + \mathcal{O}(\epsilon^2) \tag{5b}$$

where ϵ is the smallness parameter and the notation $\mathcal{O}(\epsilon^n)$ stands for all the terms of order n and higher, the zero order terms are deterministic, i.e, $\langle \mathbf{c}_i^{(0)} \rangle = \mathbf{c}_i^{(0)}$, and the first order terms, $\mathbf{c}_i^{(1)}$, are assumed to be Gaussian distributed with zero mean and covariance matrices defined by $\boldsymbol{\Sigma}_{c_{ij}} := \langle \mathbf{c}_i^{(1)} {\mathbf{c}_j^{(1)}}^T \rangle$. The optimal translation vector is assumed to have an error model with a similar structure to that of (5),

$$\mathbf{t} = \mathbf{t}^{(0)} + \epsilon\,\mathbf{t}^{(1)} + \mathcal{O}(\epsilon^2). \tag{6}$$

Conversely, the rotation matrix from $\{B\}$ to $\{A\}$ is assumed to have the special structure

$$\mathbf{R} = \exp\left(\mathbf{S}\left[\boldsymbol{\Omega}\right]\right)\mathbf{R}^{(0)} = \left[\mathbf{I} + \epsilon\,\mathbf{S}\left[\boldsymbol{\Omega}\right] + \mathcal{O}(\epsilon^2)\right]\mathbf{R}^{(0)}, \tag{7}$$

where $\boldsymbol{\Omega} \in \mathbb{R}^3$ is expected to denote the rotation error and $\mathbf{R}^{(0)}$ the true rotation matrix. With all the error models defined, the next step is to compute the expressions that define $\mathbf{t}^{(0)}$, $\mathbf{t}^{(1)}$, $\mathbf{R}^{(0)}$, and $\boldsymbol{\Omega}$ as well as their expected values and covariance matrices.

1) Rotation Uncertainty: The rotation matrix obtained through the optimization process described before belongs to the special orthogonal group $\mathrm{SO}(3)$, which yields the two constraints $\mathbf{R}^T\mathbf{R} = \mathbf{I}$ and $\det(\mathbf{R}) = 1$. It is straightforward to see that $\mathbf{R}^{(0)}$ must belong to $\mathrm{SO}(3)$ and that $\mathbf{S}\left[\boldsymbol{\Omega}\right]$ is indeed skew-symmetric, a consequence of using the error model (7). It can also be seen that the rotation matrix $\mathbf{R}^{(0)}$ is deterministic, as it is computed using the deterministic terms $\mathbf{a}_i^{(0)}$ and $\mathbf{b}_i^{(0)}$, for all $i \in \{1, \ldots, N_{\mathcal{L}}\}$, and thus, considered the true rotation matrix from $\{B\}$ to $\{A\}$.

The next steps describe the computation of the rotation error and its statistical properties, starting with some quantities associated with the closed-form solution of the optimization

problem (2). Consider the matrix that is used to compute the estimated rotation, $\mathbf{B}$. This matrix can be described in terms of its error model, using that of matrices $\mathbf{X}$ and $\mathbf{Y}$, which are a generalization of (5b) and (5a). Discarding the higher order terms in the previous expressions, it is simple to obtain the error model for $\mathbf{B}$

$$\mathbf{B} = \mathbf{B}^{(0)} + \epsilon\, \mathbf{B}^{(1)}, \tag{8}$$

with $\mathbf{B}^{(0)} = \mathbf{X}^{(0)}\mathbf{W}\mathbf{Y}^{(0)^T}$, and $\mathbf{B}^{(1)} = \mathbf{X}^{(1)}\mathbf{W}\mathbf{Y}^{(0)^T} + \mathbf{X}^{(0)}\mathbf{W}\mathbf{Y}^{(1)^T}$. From the proof of [6, Lemma], it is known that the matrix $\mathbf{BR}$ is symmetrical, and thus, using the error models (7) and (8) it is possible to show that both the deterministic and uncertain parts are also symmetric. This property is to be exploited in the determination of the rotation error, $\mathbf{\Omega}$. For that purpose, apply the skew operator to the uncertain part of $\mathbf{BR}$. This leads to $\mathbf{AS}\left[\mathbf{\Omega}\right] + \mathbf{S}\left[\mathbf{\Omega}\right]\mathbf{A}^T = \mathbf{C}^T - \mathbf{C}$, where for simplicity of notation the matrices $\mathbf{A} := \mathbf{R}^{(0)}\mathbf{B}^{(0)}$ and $\mathbf{C} := \mathbf{R}^{(0)}\mathbf{B}^{(1)}$ were introduced. Computing this expression element by element, and then rearranging the result allows to extract the underlying linear matrix equation $\boldsymbol{\mathcal{A}}\mathbf{\Omega} = \mathbf{c}$, where the matrix $\boldsymbol{\mathcal{A}} \in \mathbb{R}^{3\times 3}$ is defined as $\boldsymbol{\mathcal{A}} := [\mathrm{tr}(\mathbf{A})\,\mathbf{I}_3 - \mathbf{A}]$, and, noting that $c_{ij} \in \mathbb{R}$ is the element on the i-th row and j-th column of $\mathbf{C}$, the vector $\mathbf{c} \in \mathbb{R}^3$ is defined as

$$\mathbf{c} := \begin{bmatrix} c_{23} - c_{32} & c_{31} - c_{13} & c_{12} - c_{21} \end{bmatrix}^T. \tag{9}$$

From the linear equation now derived it is straightforward to obtain $\mathbf{\Omega}$, as long as $\boldsymbol{\mathcal{A}}$ is invertible. The next step in finding $\mathbf{\Omega}$ is then to unveil the conditions for which $\boldsymbol{\mathcal{A}}$ is invertible. The following lemma aids in achieving that goal.

Lemma 1: Let V be an Euclidean normed vector space of dimension n, $\boldsymbol{\alpha}_i \in V$, and $k_i \in \mathbb{R}$, with $i = 1, \ldots, N$. Then,

$$\sum_{j=1}^{N} k_j^2 \sum_{i=1}^{N} \|k_i \boldsymbol{\alpha}_i\|^2 \geq \left\| \sum_{i=1}^{N} k_i^2 \boldsymbol{\alpha}_i \right\|^2,$$

where the equality only applies if $\boldsymbol{\alpha}_i = \boldsymbol{\alpha}_j\ \forall i, j = 1, \ldots, N$.

Proof: The proof is done resorting to the triangle inequality and Young's inequality. It is trivial and it is omitted due to space limitations. ∎

The following theorem addresses the conditions under which $\boldsymbol{\mathcal{A}}$ is invertible.

Theorem 1: Assume that $\mathbf{b}_i^{(0)} \neq \mathbf{0}$ for all $i \in \mathcal{L}_B$. The matrix $\boldsymbol{\mathcal{A}}$ is invertible if and only if there exist at least two non-collinear landmarks $\mathbf{b}_i^{(0)}$ and $\mathbf{b}_j^{(0)}$.

Proof: The proof starts by rewriting matrix $\boldsymbol{\mathcal{A}}$ as a sum of terms involving the landmarks of both sets, as this new form provides a better insight on its properties. The necessity part of the theorem is proved by contradiction, negating the conditions of the theorem and showing that the matrix cannot be invertible. As the theorem states that there are at least two non-collinear landmarks, its negation is twofold: 1) there is only one landmark; or 2) there is an arbitrary number of landmarks, all of them collinear.

Recall that $\mathbf{A} = \mathbf{R}^{(0)}\mathbf{B}^{(0)}$, and consider matrix $\mathbf{A}$ expressed as a summation, after using the relation between the true values in analysis, $\mathbf{a}_i^{(0)} = \mathbf{R}^{(0)}\mathbf{b}_i^{(0)} + \mathbf{t}^{(0)}$,

$$\mathbf{A} = \sum_{i=1}^{N_\mathcal{L}} \sigma_i^{-2} \left[\mathbf{R}^{(0)}\mathbf{b}_i^{(0)} \left(\mathbf{R}^{(0)}\mathbf{b}_i^{(0)}\right)^T - \frac{1}{N_W} \sum_{j=1}^{N_\mathcal{L}} \sigma_j^{-2} \mathbf{R}^{(0)}\mathbf{b}_i^{(0)} \left(\mathbf{R}^{(0)}\mathbf{b}_j^{(0)}\right)^T \right], \tag{10}$$

where some algebraic manipulation was done, including isolation of the terms with $\mathbf{t}^{(0)}$. Applying the identities $\mathbf{a}^T\mathbf{b}\mathbf{I}_3 - \mathbf{a}\mathbf{b}^T = \mathbf{S}^T\left[\mathbf{b}\right]\mathbf{S}\left[\mathbf{a}\right]$ and $\mathrm{tr}(\mathbf{a}\mathbf{b}^T) = \mathbf{a}^T\mathbf{b}$, the computation of $\boldsymbol{\mathcal{A}}$ is straightforward, yielding

$$\boldsymbol{\mathcal{A}} = \sum_{i=1}^{N_\mathcal{L}} \sigma_i^{-2} \mathbf{S}^T \left[\mathbf{R}^{(0)}\mathbf{b}_i^{(0)}\right] \mathbf{S} \left[\mathbf{R}^{(0)}\mathbf{b}_i^{(0)}\right] - \frac{1}{N_W} \sum_{i,j=1}^{N_\mathcal{L}} \sigma_i^{-2}\sigma_j^{-2} \mathbf{S}^T \left[\mathbf{R}^{(0)}\mathbf{b}_j^{(0)}\right] \mathbf{S} \left[\mathbf{R}^{(0)}\mathbf{b}_i^{(0)}\right].$$

Consider that there exists only one landmark. Then it is straightforward to see that $\boldsymbol{\mathcal{A}} = \mathbf{0}_3$, which obviously proves the necessity of the existence of two or more landmarks. If $\boldsymbol{\mathcal{A}}$ is non-singular, the only solution for

$$\mathbf{u}^T\boldsymbol{\mathcal{A}}\mathbf{u} = 0, \quad \mathbf{u} \in \mathbb{R}^3, \tag{11}$$

is the trivial solution $\mathbf{u} = \mathbf{0}$. It can be shown after some algebraic manipulation that (11) is the same as

$$\sum_{i=1}^{N_\mathcal{L}} \left\| \sigma_i^{-1} \left(\mathbf{R}^{(0)}\mathbf{b}_i^{(0)}\right) \times \mathbf{u} \right\|^2 - \frac{1}{N_W} \left\| \sum_{i=1}^{N_\mathcal{L}} \sigma_i^{-2} \left(\mathbf{R}^{(0)}\mathbf{b}_i^{(0)}\right) \times \mathbf{u} \right\|^2 = 0. \tag{12}$$

noting that $\mathbf{u}\mathbf{S}^T\left[\mathbf{d}_i^*\right]\mathbf{S}\left[\mathbf{d}_i^*\right]\mathbf{u} = \left\|\mathbf{d}_i^* \times \mathbf{u}\right\|^2$ and that $\sum_{i,j} \mathbf{d}_j^* \cdot \mathbf{d}_i^* = \left(\sum_j \mathbf{d}_j^*\right) \cdot \left(\sum_i \mathbf{d}_i^*\right) = \left\|\sum_i \mathbf{d}_i^*\right\|^2$, for any arbitrary vector $\mathbf{d}_i^*$. Recall now Lemma 1. It is trivial to see that it applies, showing that the left-hand member of (12) is always greater than or equal to zero, only being zero if $\left(\mathbf{R}^{(0)}\mathbf{b}_i^{(0)}\right) \times \mathbf{u} = \left(\mathbf{R}^{(0)}\mathbf{b}_j^{(0)}\right) \times \mathbf{u}$ for all $i, j \in \mathcal{L}_B$ and $i \neq j$. This implies that the solutions of (11) are either $\mathbf{u} = \mathbf{0}$, $\mathbf{b}_i^{(0)} = \mathbf{0}\ \forall i \in \mathcal{L}_B$, or that all the landmarks are collinear. Note that the second solution contradicts the assumption that $\mathbf{b}_i^{(0)} \neq \mathbf{0}$ for all $i \in \mathcal{L}_B$. Thus, if the hypothesis of the theorem does not hold, i.e., if all the landmarks are collinear, $\boldsymbol{\mathcal{A}}$ is not invertible, concluding the necessity part of the proof. On the other hand, if there are at least two non-collinear landmarks, as the theorem states, the only solution of (11) is $\mathbf{u} = 0$, thus demonstrating the sufficiency of the condition and concluding the proof. ∎

With the insight provided by Theorem 1, it is now possible to compute the statistical properties of $\mathbf{\Omega}$, namely its expected value and covariance matrix. The expected value of the rotation error is zero as it is straightforward to show that $\mathbf{C}$ has zero mean. Given that $\mathbf{\Omega}$ is a zero mean quantity, its covariance matrix is simply given by $\mathbf{\Sigma}_\Omega = \boldsymbol{\mathcal{A}}^{-1}\langle \mathbf{c}\mathbf{c}^T \rangle \boldsymbol{\mathcal{A}}^{-1^T}$ or

$$\mathbf{\Sigma}_\Omega = \boldsymbol{\mathcal{A}}^{-1} \left[\langle (\mathbf{C} - \mathbf{C}^T)^2 \rangle - \frac{1}{2}\,\mathrm{tr}\langle (\mathbf{C} - \mathbf{C}^T)^2 \rangle\, \mathbf{I}_3 \right] \boldsymbol{\mathcal{A}}^{-1^T}. \tag{13}$$

The process of obtaining $\langle (\mathbf{C} - \mathbf{C}^T)^2 \rangle = \langle \mathbf{C}^2 \rangle - \langle \mathbf{C}\mathbf{C}^T \rangle - \langle \mathbf{C}^T\mathbf{C} \rangle + \langle \mathbf{C}^2 \rangle^T$ includes expressing $\mathbf{C}$ as a sum of terms, following the same reasoning of (10), and rearranging the obtained expressions. After some computation, it is possible to show that the three components of $\langle (\mathbf{C} - \mathbf{C}^T)^2 \rangle$ are

$$\langle \mathbf{C}\mathbf{C} \rangle = \sum_{i,j=1}^{N_\mathcal{L}} \sigma_j^{-2} \left[\mathbf{R}^{(0)} \mathbf{\Sigma}_{b_{ij}} \mathbf{R}^{(0)^T} \bar{\mathbf{a}}_i^{(0)} \bar{\mathbf{a}}_j^{(0)^T} + \mathbf{R}^{(0)}\mathbf{b}_i^{(0)}\mathbf{b}_j^{(0)^T}\mathbf{R}^{(0)^T} \langle \bar{\mathbf{a}}_i^{(1)} \bar{\mathbf{a}}_j^{(1)^T} \rangle \right],$$

$$\langle \mathbf{C}\mathbf{C}^T \rangle = \sum_{i,j=1}^{N_\mathcal{L}} \sigma_i^{-2}\sigma_j^{-2} \Big[\mathbf{R}^{(0)} \mathbf{\Sigma}_{b_{ij}} \mathbf{R}^{(0)^T} \bar{\mathbf{a}}_i^{(0)^T} \bar{\mathbf{a}}_j^{(0)} + \mathbf{R}^{(0)} \mathbf{b}_i^{(0)} \mathbf{b}_j^{(0)^T} \mathbf{R}^{(0)^T} \operatorname{tr}\langle \bar{\mathbf{a}}_i^{(1)} \bar{\mathbf{a}}_j^{(1)^T} \rangle \Big],$$

$$\langle \mathbf{C}^T\mathbf{C} \rangle = \sum_{i,j=1}^{N_\mathcal{L}} \sigma_i^{-2}\sigma_j^{-2} \Big[\mathbf{b}_i^{(0)^T} \mathbf{b}_j^{(0)} \langle \bar{\mathbf{a}}_i^{(1)} \bar{\mathbf{a}}_j^{(1)^T} \rangle + \operatorname{tr}(\mathbf{\Sigma}_{b_{ij}}) \bar{\mathbf{a}}_i^{(0)} \bar{\mathbf{a}}_j^{(0)^T} \Big],$$

with

$$\langle \bar{\mathbf{a}}_i^{(1)} \bar{\mathbf{a}}_j^{(1)^T} \rangle = \mathbf{\Sigma}_{a_{ij}} + \frac{1}{N_W^2} \sum_{r,s=1}^{N_\mathcal{L}} \sigma_r^{-2}\sigma_s^{-2} \mathbf{\Sigma}_{a_{rs}} - \frac{1}{N_W} \sum_{r=1}^{N_\mathcal{L}} \sigma_r^{-2} \left(\mathbf{\Sigma}_{a_{ir}} + \mathbf{\Sigma}_{a_{rj}} \right),$$

where $\bar{\mathbf{a}}_i^{(.)} \in \mathbb{R}^3$ is the deterministic or uncertain part, depending on whether the superscript is respectively (0) or (1), of a landmark in $\mathcal{L}_A$ to which are subtracted the coordinates of the weighted centroid of the set, i.e., $\bar{\mathbf{a}}_i^{(.)} := \mathbf{a}_i^{(.)} - \frac{1}{N_W} \sum_{j \in \mathcal{L}_A} \sigma_i^{-2} \mathbf{a}_j^{(.)}$. In these computations, it is assumed that the uncertainty of the landmarks from one set is independent from the ones in the other. Note that, as the true rotation $\mathbf{R}^{(0)}$ is unknown, a possible approximation is to use $\mathbf{R}^*$ in these computations.

2) Translation Uncertainty: The optimal translation between frames is given by (3), and the associated error model is assumed to be (6). Using this information along with the error models for the landmarks in both sets, defined in (5), it is possible to expand (3) to obtain

$$\mathbf{t}^{(0)} = \frac{1}{N_W} \sum_{i=1}^{N_\mathcal{L}} \sigma_i^{-2} \left(\mathbf{a}_i^{(0)} - \mathbf{R}^{(0)} \mathbf{b}_i^{(0)} \right),$$

and

$$\mathbf{t}^{(1)} = \frac{1}{N_W} \sum_{i=1}^{N_\mathcal{L}} \sigma_i^{-2} \left(\mathbf{a}_i^{(1)} - \mathbf{S}\left[\mathbf{\Omega}\right] \mathbf{R}^{(0)} \mathbf{b}_i^{(0)} - \mathbf{R}^{(0)} \mathbf{b}_i^{(1)} \right). \quad (14)$$

It is easy to confirm that $\mathbf{t}^{(0)}$ is deterministic and that $\mathbf{t}^{(1)}$ has zero mean, noting that all the non-deterministic quantities involved have zero mean. An approximate expression for the covariance matrix may be obtained by expanding $\mathbf{t}^{(1)}$ according to (14), using the cross product property $\mathbf{S}\left[\mathbf{a}\right]\mathbf{b} = -\mathbf{S}\left[\mathbf{b}\right]\mathbf{a}$ to extract the $\mathbf{\Omega}$ from the skew-symmetric matrix, and neglecting the cross covariance terms between the rotation error and the landmarks of both sets, i.e., the terms with combinations of $\mathbf{\Omega}$ and $\mathbf{a}_i^{(1)}$, and $\mathbf{\Omega}$ and $\mathbf{b}_i^{(1)}$. This yields

$$\mathbf{\Sigma}_t \approx \frac{1}{N_W^2} \sum_{i,j=1}^{N_\mathcal{L}} \sigma_i^{-2}\sigma_j^{-2} \Big(\mathbf{\Sigma}_{a_{ij}} + \mathbf{R}^{(0)} \mathbf{\Sigma}_{b_{ij}} \mathbf{R}^{(0)^T} + \mathbf{S}\left[\mathbf{R}^{(0)}\mathbf{b}_i^{(0)}\right] \mathbf{\Sigma}_\Omega \mathbf{S}^T \left[\mathbf{R}^{(0)}\mathbf{b}_j^{(0)}\right] \Big), \quad (15)$$

where all the cross terms between landmarks of different sets were omitted, as they are assumed to be independent.

IV. Inertial Trajectory and Map Estimation

This section addresses the problem of obtaining an estimate of the pose of the vehicle and of the inertial map, by formulating an optimization problem with a solution that corresponds to an estimate of the transformation between the body-fixed frame $\{B\}$ and the inertial frame $\{I\}$, yielding the ITM algorithm here proposed. An error function is defined and then used to construct a functional for the optimization problem. The algorithm builds on the derivation of the Subsection III-A and the uncertainty characterization of III-B.

A. Formulation and Solution of the Problem

The problem of estimating the transformation between the body-fixed and inertial frames, defined by the orientation and position of the vehicle in frame $\{I\}$, ${}^I\hat{\mathbf{p}}_k \in \mathbb{R}^3$ and $\hat{\mathbf{R}}_k \in \mathrm{SO}(3)$, respectively, is analogous to the Procrustes problem proposed in the previous section. The optimization problem treated in Section III assumes that the landmarks in both sets are known before the computation of the transformation between frames. However, the sensor-based SLAM filter only outputs the body-fixed map, $\mathcal{I}_{B_k}$, and the inertial set $\mathcal{I}_{I_k}$ can only be computed using the transformation between frames, as the following update equation for all $i \in \{1, \ldots, N_M\}$ shows

$${}^I\hat{\mathbf{p}}_{i_k} = \hat{\mathbf{R}}_k \hat{\mathbf{p}}_{i_k} + {}^I\hat{\mathbf{p}}_k. \quad (16)$$

This algebraic loop may be averted if it is noticed that, as the landmarks in $\mathcal{I}_{I_k}$ are static, there is also a correspondence between ${}^I\hat{\mathbf{p}}_{i_{k-1}}$ and $\hat{\mathbf{p}}_{i_k}$, $i \in \{1, \ldots, N_M\}$. This step is of the utmost importance in the design of the algorithm, and yields the error function ${}^I\mathbf{e}_{i_k} = {}^I\hat{\mathbf{p}}_{i_{k-1}} - \hat{\mathbf{R}}_k \hat{\mathbf{p}}_{i_k} - {}^I\hat{\mathbf{p}}_k$, that represents the error between the previous estimate of the inertial landmark $i \in \mathcal{I}_{I_{k-1}}$ and its sensor-based homologous at time k, rotated and translated with the estimated transformation. The pair $\left(\hat{\mathbf{R}}_k, {}^I\hat{\mathbf{p}}_k\right)$ can be obtained using the optimization problem (2), considering the cost functional $G\left(\hat{\mathbf{R}}_k, {}^I\hat{\mathbf{p}}_k\right) = \sum_{i=1}^{N_T} \sigma_{i_k}^{-2} {}^I\mathbf{e}_{i_k}$. The ITM algorithm uses only a subset of N_T more recent landmarks to make the algorithm more computationally efficient, while maintaining a minimum N_T for statistical consistency and numerical robustness. The estimates of the vehicle position and attitude are then computed using (3) and (4), respectively, and their uncertainties are those derived in Subsection III-B. The inertial map estimate at instant k is computed using the update equation (16), following the computation of the optimal translation and rotation using the sensor-based map estimate of instant k and the inertial estimate of the previous iteration, enabling the real-time estimation of the inertial map.

The algorithm is initialized with the pose of the vehicle that is known at $k = 0$. This yields ${}^I\hat{\mathbf{p}}_{i_0} = \mathbf{R}_0 \hat{\mathbf{p}}_{i_0} + {}^I\mathbf{p}_0$ and $\mathbf{\Sigma}_{{}^I p_{ij_0}} = \mathbf{R}_0 \mathbf{\Sigma}_{p_{ij_0}} \mathbf{R}_0^T$.

The work presented in this paper, including the estimates for the vehicle pose, given by (3) and (4), and the update equation (16), allows the real-time computation of the vehicle trajectory and the inertial map. However, the ITM algorithm here described assumes the knowledge of the uncertainty of both the inertial and sensor-based landmark estimates. The latter is directly provided by the filter in [2], but the former is yet to be described. The scope of this section is also to provide approximate uncertainty descriptions of the estimates provided by this algorithm, using perturbation theory. A similar approach for the bidimensional case is hinted in [4].

B. Inertial Map Uncertainty

The final step in the process of studying the uncertainty description of the algorithm is computing $\mathbf{\Sigma}_{{}^I p_{ij_k}}$, for all

$i, j \in \mathcal{I}_{I_k}$. Recall that the inertial map estimate is calculated with the update equation (16) which can be combined with the error models (5b), (6) and (8) to write,

$$
{}^{I}\hat{\mathbf{p}}_{i_k} = {}^{I}\hat{\mathbf{p}}_{k}^{(0)} + \mathbf{R}_{k}^{(0)}\hat{\mathbf{p}}_{i_k}^{(0)} + \epsilon\left({}^{I}\hat{\mathbf{p}}_{k}^{(1)} + \mathbf{S}\left[\boldsymbol{\Omega}_k\right]\mathbf{R}_{k}^{(0)}\hat{\mathbf{p}}_{i_k}^{(0)} + \mathbf{R}_{k}^{(0)}\hat{\mathbf{p}}_{i_k}^{(1)}\right),
$$

while ignoring second or higher order terms. Once again, it is quite simple to confirm that ${}^{I}\hat{\mathbf{p}}_{i_k}^{(0)}$ is deterministic and that ${}^{I}\hat{\mathbf{p}}_{i_k}^{(1)}$ has zero mean. Thus, the covariance matrix of the position estimate may be approximated by

$$
\begin{aligned}
\boldsymbol{\Sigma}_{{}^{I}p_{i_j k}} \approx\ & \boldsymbol{\Sigma}_{{}^{I}p_k} + \mathbf{R}_{k}^{(0)}\boldsymbol{\Sigma}_{p_{i_j k}}{\mathbf{R}_{k}^{(0)}}^{T} \\
& + \mathbf{S}\left[\mathbf{R}_{k}^{(0)}\hat{\mathbf{p}}_{i_k}^{(0)}\right]\boldsymbol{\Sigma}_{\Omega_k}\mathbf{S}^{T}\left[\mathbf{R}_{k}^{(0)}\hat{\mathbf{p}}_{j_k}^{(0)}\right] \\
& + \mathbf{S}^{T}\left[\mathbf{R}_{k}^{(0)}\hat{\mathbf{p}}_{i_k}^{(0)}\right]\boldsymbol{\Sigma}_{{}^{I}p_k\Omega_k}^{T} + \boldsymbol{\Sigma}_{{}^{I}p_k\Omega_k}\mathbf{S}\left[\mathbf{R}_{k}^{(0)}\hat{\mathbf{p}}_{j_k}^{(0)}\right],
\end{aligned}
$$

where all the cross terms between inertial and sensor-based landmarks were omitted, as they are assumed to be zero and, as before, the cross covariance terms between the rotation error and the landmarks were neglected. Furthermore, the cross covariance terms between the vehicle position and the landmarks (both inertial and sensor-based) were also neglected. The covariances $\boldsymbol{\Sigma}_{{}^{I}p_k}$ and $\boldsymbol{\Sigma}_{\Omega_k}$ are computed using (15) and (13), respectively. The matrix $\boldsymbol{\Sigma}_{{}^{I}p_k\Omega_k} := \langle {}^{I}\hat{\mathbf{p}}_{k}^{(1)}\boldsymbol{\Omega}_{k}^{T}\rangle = \langle {}^{I}\hat{\mathbf{p}}_{k}^{(1)}\mathbf{c}_{k}^{T}\rangle\boldsymbol{\mathcal{A}}^{-1}$ denotes the cross covariance of the translation and rotation estimates, whose columns are related to linear combinations of $\langle {}^{I}\hat{\mathbf{p}}_{k}^{(1)}c_{lm}\rangle$, $l, m \in \{1, 2, 3\}$ (recall the definition of $\mathbf{c}$ in (9)). This covariance is approximately given by

$$
\begin{aligned}
\langle {}^{I}\hat{\mathbf{p}}_{k}^{(1)}c_{lm}\rangle \approx \frac{1}{N_{W_k}}\sum_{i,j=1}^{N_T}\sigma_{i_k}^{-2}\sigma_{j_k}^{-2}\Big[& \boldsymbol{\Sigma}_{{}^{I}p_{i_j k}}\mathbf{1}_m\mathbf{1}_l^{T}\mathbf{R}_{k}^{(0)}\hat{\mathbf{p}}_{j_k}^{(0)} \\
& - \frac{1}{N_{W_k}}\sum_{r=1}^{N_T}\sigma_r^{-2}\boldsymbol{\Sigma}_{{}^{I}p_{i r_k}}\mathbf{1}_m\mathbf{1}_l^{T}\mathbf{R}_{k}^{(0)}\hat{\mathbf{p}}_{j_k}^{(0)} \\
& - \mathbf{R}_{k}^{(0)}\boldsymbol{\Sigma}_{p_{i_j k}}{\mathbf{R}_{k}^{(0)}}^{T}\mathbf{1}_l\mathbf{1}_m^{T}\mathbf{a}_{j_k}^{(0)}\Big],
\end{aligned}
$$

where all the usual assumptions were taken into account, $\mathbf{1}_m := \begin{bmatrix}\mathbf{0}_{1\times(m-1)} & 1 & \mathbf{0}_{1\times(3-m)}\end{bmatrix}^{T}$, and $\mathbf{a}_{i_k}^{(0)}$ is the equivalent of $\bar{\mathbf{a}}_{i}^{(0)}$ for this problem.

Remark 1: The computation of the cross-covariances is a highly nonlinear problem where, for example, $\boldsymbol{\Sigma}_{{}^{I}p_i p_j}$ depends on itself. That is the reason why they are neglected in this work.

Remark 2: In this procedure an inertial landmark is only updated if the associated uncertainty decreases. Thus, in each iteration the candidate inertial landmarks covariance matrix is computed, and the trace of each $\boldsymbol{\Sigma}_{{}^{I}p_{i_k}}$ is compared to its previous value. If the uncertainty is raised, then the old covariance is kept and $\boldsymbol{\Sigma}_{{}^{I}p_{i j_{k+1}}} = \mathbf{0}$ for all $j \neq i$.

V. Simulation Results

This section provides simulation results for the performance evaluation of the overall algorithm, which includes the sensor-based SLAM filter described in Section II and the inertial trajectory and map estimation algorithm proposed in this paper. The simulated environment consists of 70 landmarks spread throughout a 16m×16m×3m map, including a closed 2m wide corridor in the outer borders of the map. The trajectory is simply a loop through the corridors at half-height, with the vehicle starting on the floor. The simulation starts with the vehicle stopped for 50 seconds, which then takes off and circles through the map for around 230 seconds at an average speed of 0.45 m/s, making a whole loop around the corridor. The zero-mean noise added to the angular velocity measurements is Gaussian-distributed with a standard deviation of $\sigma_{\omega_m} = 5 \times 10^{-4}$ rad/s in each coordinate and the noise included in the landmark observations is also zero-mean Gaussian white noise with a standard deviation of $\sigma_y = 10^{-3}$ m. Figure 1 presents the norm of the estimation error and the standard deviation of the position (Fig. 1(a)) and attitude (Fig. 1(b)) of the vehicle. It can be seen that the position error is kept under 10 cm and the rotation error, expressed by $\left\|\tilde{\mathbf{R}}_k\right\| = \arccos\left(\frac{1}{2}\left(\mathrm{tr}\left(\hat{\mathbf{R}}_k{}^{T}\mathbf{R}_k\right) - 1\right)\right)$, remains under 1°. Notice the convergence of the uncertainty when the vehicle is stopped and 5 landmarks are visible, i.e., the observability conditions are satisfied. The estimation error norm and the standard deviation of the first 10 landmarks is show in Fig. 2(a) and Fig. 2(b), respectively. Note also that the uncertainty never increases, as explained in Section IV. Finally, the estimated trajectory and map after a complete loop are shown in Fig. 3. The blue line is the estimated trajectory, and the red star denotes the position of the vehicle at the time. Figure 3(b) shows a detail of the upper-right part of the map as seen from above, this time with the 95% confidence bounds of the landmarks estimates, represented by the coloured ellipsoids.

This simulation was designed to show the performance of the algorithm as a whole, allowing the demonstration of its convergence and consistency. In the results here presented, the validity of the optimization-based solution found in

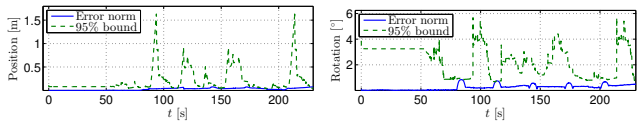

(a) Position. (b) Rotation.

Fig. 1. Error norm and 2σ bounds of the position and rotation matrix estimates.

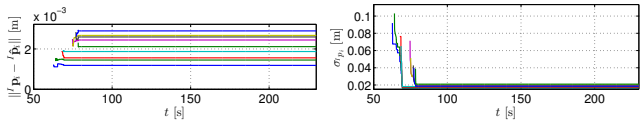

(a) Estimation error norm. (b) Standard deviation.

Fig. 2. Error and standard-deviation of the 10 first landmarks.

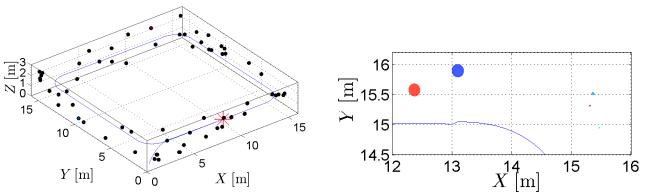

(a) Full map. (b) Map detail.

Fig. 3. Estimated inertial map at $t = 191$ s.

Section III may be evaluated, as well as the consistency of the uncertainty characterization derived here.

VI. Preliminary Experimental Results

The simulation results were consolidated by a preliminary experiment at the Sensor-Based Cooperative Robotics Research Laboratory - SCORE Lab of the Faculty of Science and Technology of the University of Macau.

The experimental setup consists of an *AscTec Pelican* quadrotor, which is equipped with an *Intel Atom* processor board, and into which was added a *Microstrain 3DM-GX3-25* inertial measurement unit working at 200Hz and a *Microsoft Kinect* camera, at 30Hz. The experiment consisted in moving the quadrotor inside a $6\mathrm{m}\times6\mathrm{m}$ room (usable area of $16\mathrm{m}^2$) equipped with a *VICON* motion capture system. An implementation of SURF [11] was employed to detect landmarks. In the first 15 seconds the vehicle was stopped and in the remaining time it was moved in a small lap around the room. Figure 4 shows the comparison of the estimation of the inertial trajectory (in red) with the ground truth provided by the *VICON*, the dashed blue line. It can be seen that the estimated trajectory follows very closely the true trajectory of the vehicle, never being more than 20 centimeters off, except after the first 30 seconds, where less observations were available as it can be seen in Fig. 6. Figure 5 compares the ground truth data with the estimation of the yaw angle of the vehicle. Again, the estimation follows within reasonable accuracy the ground truth. Finally, the evolution of the number of landmarks

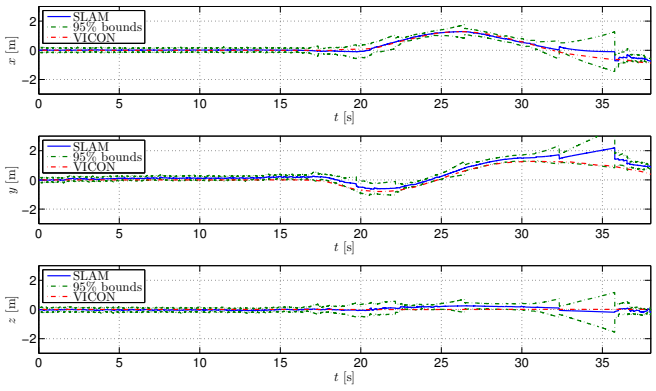

Fig. 4. Time evolution of the real and estimated trajectory.

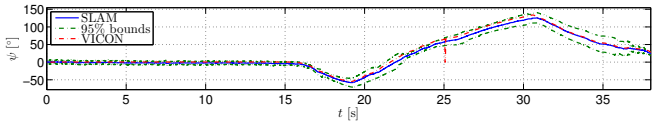

Fig. 5. The estimated yaw against the ground truth data.

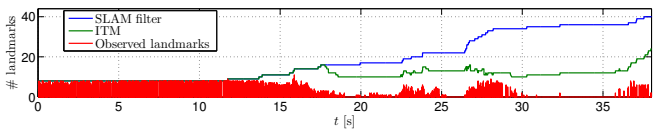

Fig. 6. Evolution of the number of landmarks stored (in blue), the number of landmarks used for inertial estimation (in green), and the number of visible landmarks (in red).

involved in the algorithm is shown. The number of landmarks in the SLAM filter state is presented in blue, the number of landmarks used in the ITM algorithm to compute the optimal transformation is the green dashed line, and the number of visible landmarks in each observation instant is shown in red. Note that, after the first 30 seconds, the refresh rate of the observations is reduced drastically, due to technical issues with the equipment, while the number of landmarks observed is also small. This explains the degradation in the estimation that occurs around that time.

VII. Conclusions and Future Work

This paper presented an optimization-based algorithm to solve the orthogonal Procrustes problem, fully characterized uncertainty-wise, that is part of a novel algorithm for Simultaneous Localization and Mapping. The complete algorithm provides estimates of the landmark map and of the attitude and position of the vehicle in both the body-fixed and inertial frames. Building on the body-fixed map provided by the sensor-based filter, the problem of obtaining the inertial trajectory and map was formulated using an orthogonal Procrustes problem approach, and a statistical description associated with the closed form solution is also proposed. Furthermore, the performance and consistency of the algorithm were validated in simulation, while preliminary experimental results, with ground truth data, showed also the good performance of the SLAM algorithm as a whole.

Future work includes the design of an improved experimental setup to further demonstrate the capabilities of the proposed overall SLAM algorithm.

References

[1] H. Durrant-Whyte and T. Bailey, "Simultaneous Localisation and Mapping (SLAM): Part I The Essential Algorithms," *IEEE Robotics & Automation Magazine*, vol. 13, no. 2, pp. 99–110, 2006.

[2] P. Lourenço, B. J. Guerreiro, P. Batista, P. Oliveira, and C. Silvestre, "Preliminary Results on Globally Asymptotically Stable Simultaneous Localization and Mapping in 3-D," in *American Control Conference 2013*, June 2013, accepted.

[3] B. Guerreiro, P. Batista, C. Silvestre, and P. Oliveira, "Sensor-based Simultaneous Localization and Mapping - Part I: GAS Robocentric Filter," in *Proc. of the 2012 American Control Conference*, Montréal, Canada, Jun. 2012, pp. 6352–6357.

[4] ——, "Sensor-based Simultaneous Localization and Mapping - Part II: Online Inertial Map and Trajectory Estimation," in *Proc. of the 2012 American Control Conference*, Montréal, Canada, Jun. 2012, pp. 6334–6339.

[5] C. Goodall, "Procrustes Methods in the Statistical Analysis of Shape," *Journal of the Royal Statistical Society. Series B (Methodological)*, vol. 53, no. 2, pp. 285–339, 1991.

[6] S. Umeyama, "Least-squares estimation of transformation parameters between two point patterns," *IEEE Transactions On Pattern Analysis and Machine Intelligence*, vol. 13, no. 4, pp. 376–380, 1991.

[7] B. K. P. Horn, H. Hilden, and S. Negahdaripour, "Closed-form solution of absolute orientation using orthonormal matrices," *Journal of the Optical Society America*, vol. 5, no. 7, pp. 1127–1135, 1988.

[8] R. Sibson, "Studies in the robustness of multidimensional scaling: Perturbational analysis of classical scaling," *Journal of the Royal Statistical Society. Series B (Methodological)*, vol. 41, no. 2, pp. 217–229, 1979.

[9] ——, "Studies in the robustness of multidimensional scaling: Procrustes statistics," *Journal of the Royal Statistical Society. Series B (Methodological)*, vol. 40, no. 2, pp. 234–238, 1978.

[10] K. Arun, T. S. Huang, and S. D. Blostein, "Least-Squares Fitting of Two 3-D Point Sets," *IEEE Transactions on Pattern Analysis and Machine Intelligence*, vol. PAMI-9, no. 5, pp. 698–700, 1987.

[11] H. Bay, A. Ess, T. Tuytelaars, and L. V. Gool, "Speeded-Up Robust Features (SURF)," *Computer Vision and Image Understanding*, vol. 110, no. 3, pp. 346 – 359, 2008, Similarity Matching in Computer Vision and Multimedia.